

## Ultra High-speed Observation of Dynamic Fracture using C. G.S. Methods under Mix-mode Impact Load

T. Nishioka<sup>1</sup>, M.Kogame<sup>2</sup>, T. Fujimoto<sup>1</sup> and G. Okamoto<sup>1</sup>

### Summary

In this study, we observed C.G.S. fringe pattern of dynamic fracture under impact load by an ultra high-speed CCD video camera, and stress intensity factors  $K_I$ ,  $K_{II}$  are evaluated from the experimental measurements. From the evaluation of stress intensity factors, local mode I condition is observed during crack propagation. On the other hand, concentrated load is obtained by the experimental devices in this study. We suggest the least square method to estimate loading value based on the C.G.S. fringe pattern analyses.

### Introduction

The clarification of mechanism for the shear dominated fracture is one of very important problems in the fracture mechanics field. The contact of crack surfaces may be caused in this type of fracture. In our previous study[1], we observed distributions of principal stress sum gradient near crack tip by the Coherent Gradient Sensing (C.G.S.) method[2]. The stress intensity factor  $K_I$  evaluated for high-speed straight crack propagation under mode I load. However, the measurement method to evaluate  $K_I$  and  $K_{II}$  was not established for nonstraight crack propagation.

In this study, we observe C.G.S. fringe patterns for mix-mode fracture under impact load method using ultra high-speed video camera. The measurement of stress intensity factors is restricted for straight crack propagation in our previous study. And more, to measure load value, we focused on C.G.S. fringe pattern near loading point.

### Estimate of Stress Intensity Factor Based on C.G.S. Method

We use the C.G.S. method[2] to visualize principal stress sum gradient distribution near the crack tip. The C.G.S. fringe pattern is equivalent to contour lines of principal stress sum gradient distribution on the specimen. The equation (1) expresses the relation between fringe order 'n' in the C.G.S. images and stress gradient:

$$\frac{\partial(\sigma_1 + \sigma_2)}{\partial X_i} = \frac{np}{c_o t \Delta} \quad (1)$$

where,  $c_o$ ,  $t$ ,  $\sigma_1$ ,  $\sigma_2$ ,  $p$ ,  $\Delta$ , and  $X_i$  denote optical constant of specimen's material, thickness of specimen, principal stress components, pitch of grating, distance of two grating planes, and grid direction, respectively.

---

<sup>1</sup>Professor, Kobe Univ., Japan

<sup>2</sup>Gradient Student, Kobe Univ., Japan

In the case of stationary crack tip, under mix-mode load the equation (2) shows the relation between the principal stress sum gradient and stress intensity factors:

$$\frac{\partial(\sigma_1 + \sigma_2)}{\partial X_i} = -\frac{K_I}{\sqrt{2\pi}} r^{-\frac{3}{2}} \cos \frac{3}{2}\theta + \frac{K_{II}}{\sqrt{2\pi}} r^{-\frac{3}{2}} \sin \frac{3}{2}\theta \quad (2)$$

where,  $r$  and  $\theta$  denote the near field point location based on the crack tip polar coordinate system.

From the equation (1) and (2), we can derive the equation (3) which shows relation between C.G.S. fringe pattern and the stress gradient:

$$\frac{np}{c_{ot}\Delta} = \frac{K_I}{\sqrt{2\pi}} r^{-\frac{3}{2}} \cos \frac{3}{2}\theta + \frac{K_{II}}{\sqrt{2\pi}} r^{-\frac{3}{2}} \sin \frac{3}{2}\theta \quad (3)$$

In the case of propagating crack tip, we formulate the relation between the principal stress sum gradient near the crack tip and the C.G.S. fringe pattern. The equation (4) is a sum of principal stresses  $\sigma_1 + \sigma_2$  which considered influence of crack propagating velocity was provided by T.Nishoka and et.al. [3]:

$$\begin{aligned} \sigma_1 + \sigma_2 &= \frac{2(\beta_2^2 - \beta_1^2)}{\sqrt{2\pi}} r_1^{-\frac{1}{2}} \left\{ K_I B_I(c) \cos \frac{1}{2}\theta_1 - K_{II} B_{II}(c) \sin \frac{1}{2}\theta_1 \right\} \\ \text{On } \beta_1^2 &= 1 - c^2/c_d^2 \quad \beta_2^2 = 1 - c^2/c_s^2 \\ B_I(c) &= \frac{1 + \beta_2^2}{4\beta_1\beta_2 - (1 + \beta_2^2)^2} \quad B_{II}(c) = \frac{2\beta_2}{4\beta_1\beta_2 - (1 + \beta_2^2)^2} \\ \theta_1 &= \tan^{-1} \frac{\beta_1 y}{x} \quad r_1^2 = x^2 + \beta_1^2 y^2 \end{aligned} \quad (4)$$

where,  $c$ ,  $c_d$  and  $c_s$  denote crack propagation velocity, dilatational wave speed and shear wave speed.  $x$  and  $y$  denote the near field point location based on the crack tip orthogonal coordinate system. The equation (5) is obtained by differentiating the equation (4) in X coordinate.

$$\begin{aligned} \frac{\partial(\sigma_1 + \sigma_2)}{\partial X_1} &= -\frac{K_I B_I(C)}{2\sqrt{2\pi}} (\beta_1^2 - \beta_2^2) r_1^{-\frac{3}{2}} P + \frac{K_{II} B_{II}(C)}{2\sqrt{2\pi}} (\beta_1^2 - \beta_2^2) r_1^{-\frac{3}{2}} Q \\ \text{On } P &= \cos \left( \frac{3}{2}\theta_1 + \theta_x \right) + \cos \left( \frac{3}{2}\theta_1 - \theta_x \right) - \beta_1 \left\{ \cos \left( \frac{3}{2}\theta_1 + \theta_x \right) - \cos \left( \frac{3}{2}\theta_1 - \theta_x \right) \right\} \\ Q &= \sin \left( \frac{3}{2}\theta_1 + \theta_x \right) + \sin \left( \frac{3}{2}\theta_1 - \theta_x \right) - \beta_1 \left\{ \sin \left( \frac{3}{2}\theta_1 + \theta_x \right) - \sin \left( \frac{3}{2}\theta_1 - \theta_x \right) \right\} \end{aligned} \quad (5)$$

where,  $\theta_x$  denotes an angle with a direction of propagating crack tip and X coordinate.

From the equation (1) and (5), we can derive the equation (6) which shows relation between the C.G.S. fringe pattern and the stress intensity factor.

$$\frac{np}{c_o t \Delta} = -\frac{K_I B_I(C)}{2\sqrt{2\pi}}(\beta_1^2 - \beta_2^2)r_1^{-\frac{3}{2}}P + \frac{K_{II} B_{II}(C)}{2\sqrt{2\pi}}(\beta_1^2 - \beta_2^2)r_1^{-\frac{3}{2}}Q \quad (6)$$

where, unknown values are  $n$ ,  $K_I$  and  $K_{II}$ . These parameters are evaluated by the least square method, in which data at many measurement points is used.

### Experimental Setup and Measurement of Stress Intensity Factors

Fig.1 shows the specimen geometry. The specimen's material is PMMA, which's Young's modulus is 2.948 [GPa], Poisson's ratio is 0.329 and mass density is 1190 [kg/m<sup>3</sup>].

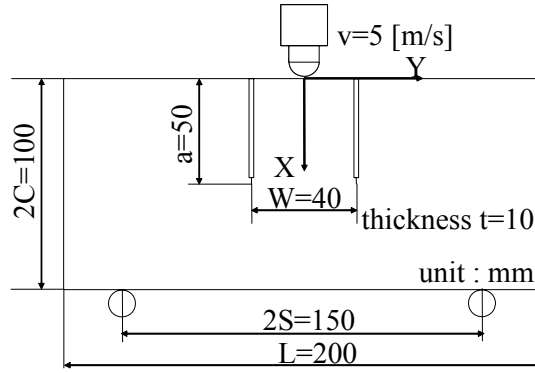


Figure 1: specimen geometry

As a dynamic loading fracture experimental, we dropped a striker so that striker's speed became 5 [m/s]. We observed dynamic stress gradient distributions near crack tip and the C.G.S. method. In order to recording the C.G.S. images, we used the ultra high-speed CCD camera and the argon pulse laser, which are synchronized. This camera can record 102 images with maximum recording velocity of one million frames per second. Pitch of gratings 'p' is 0.025 [mm/line] and distance of gratings 'Δ' is 70 [mm].

Fig.2 shows C.G.S. images on dynamic crack propagating. A photography range is located on the lower left part of the specimen. The image recording started when the striker contacts the specimen. Fig.3 shows stress intensity factor histories. Mode II condition dominates the near-field deformation of the stationary crack tip. For the propagating crack tip, mode II effect is disappeared and mode I condition is observed from the measurement of stress intensity factors. This phenomenon indicates the local symmetry.

Next, we focused on near loading point. At first, we considered on static load. For pure bending of straight bars without cracks, the equation (7) shows principal

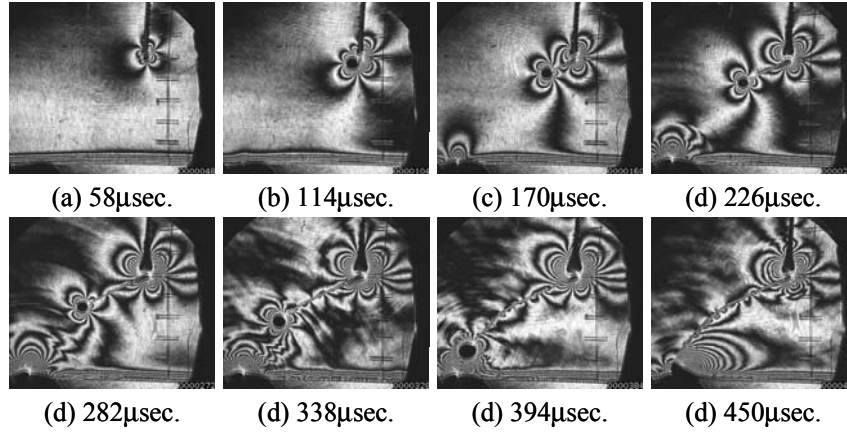


Figure 2: High-speed photographs of dynamically fracturing specimen

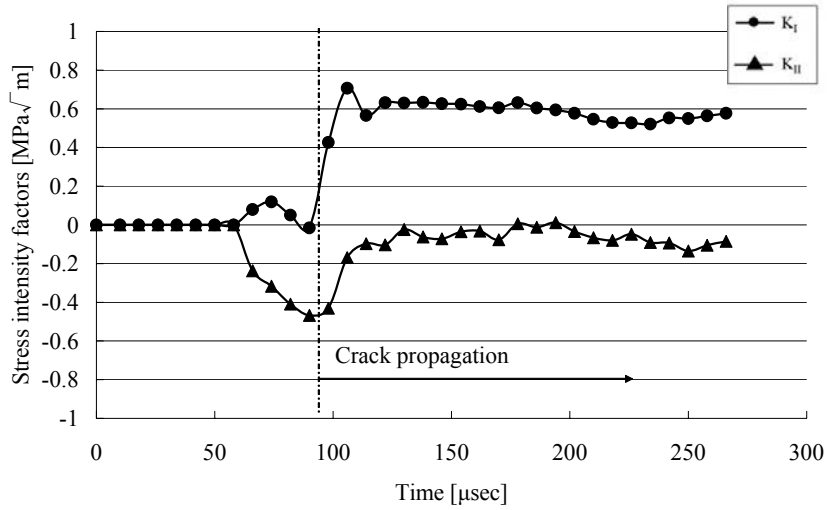


Figure 3: Stress intensity factors history

stress sum that provided by M.M.Frocht [4]:

$$\sigma_1 + \sigma_2 = \frac{-2F}{\pi t} \left\{ \frac{xy^2 + x^3}{(x^2 + y^2)} + \frac{3\pi}{8C^3}(S - |y|)(x - C) \right\} \quad (7)$$

where, F denotes concentrated load. c, s and t are defined in fig.1. We got equation (8) by differentiating equation (7) in x coordinate.

$$\frac{\partial(\sigma_1 + \sigma_2)}{\partial X} = \frac{-2F}{\pi t} \left\{ \frac{-x^2 + y^2}{(x^2 + y^2)^2} + \frac{3\pi}{8C^3}(S - |y|) \right\} \quad (8)$$

From the equation (1) and (8), we can show the equation (9) which is the equation to evaluate the load value from C.G.S. fringe pattern.

$$F = \left[ \frac{-2}{\pi t} \left\{ \frac{-x^2 + y^2}{(x^2 + y^2)^2} \right\} + \frac{3\pi}{8C^3} (S - |y|)^{-1} \right] \times \frac{np}{c_0 t \Delta} \quad (9)$$

where, unknowns values are n, and F, likewise stress intensity factor measurement, we used least square method.

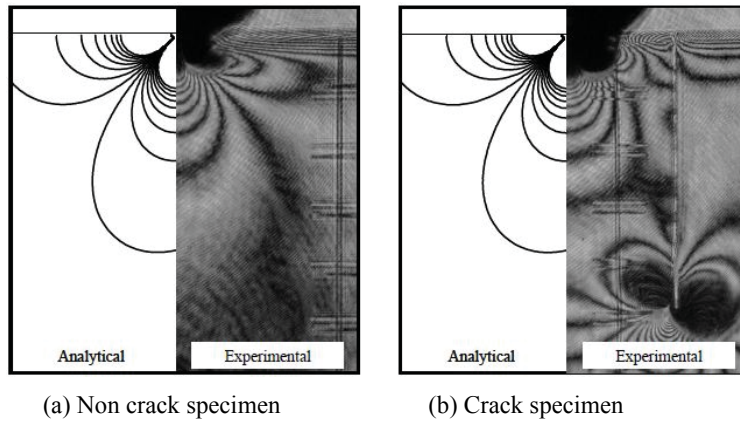


Figure 4: Comparison of analytical and experimental C.G.S. fringe pattern near loading point

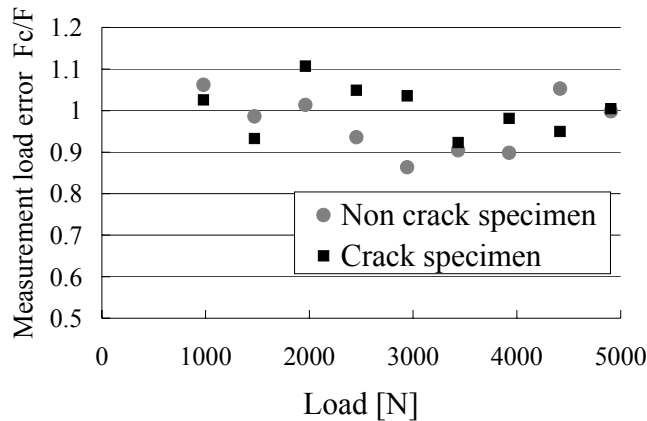


Figure 5: measurement load error

Fig.4 shows comparison of analytical and experimental C.G.S fringe pattern near loading point. In fig.4, quasi-static load 3924[N] is provided by the loading device, as an example. From the experimental measurements, load values ‘Fc’ are estimated by using the least square method based on eq.(9). ‘F’ is the exact load

value, which is indicated by the loading device. Good agreements of  $F_c$  and  $F$  are shown in fig.5. Fig.5 shows that we can measure load value with approximately 10% error from the C.G.S. fringe pattern.

### Conclusions

Based on the theory of C.G.S. method, we formulate the least square method to evaluate stress intensity factor  $K_I$  and  $K_{II}$  for stationary and propagating crack tip. These do not ask it whether it is mix-mode, going straight propagating and propagating or stationary. Mix-mode condition is dominated for the stationary crack tip. During crack propagating, mode I condition is observed from the measurement of stress intensity factor, and these results indicate the local symmetry condition for the propagating crack tip. Next, we measure loading value from C.G.S. fringe pattern.

### References

1. T.Nishioka, K.Ymaguchi, Y.Sakaguchi, H.Furuta, K.Sakakura, T.Fujimoto, (2005): "Study on High-speed Crack Propagation Phenomena under Static Multiple Loading System", *Journal of Journal of the Japanese Society for Experimental Mechanics*, Vol5, No.4, pp.367-372.
2. Hareesh V.Tippur, Sridhar Krishnaswamy, and Ares J.Rosakis, (1989): "A Coherent Gradient Sensor for Crack Tip Deformation Measurements : Analysis and Experimental Result", *SM Reports*89-1
3. T.Nishioka, and S.N.Atluri, (1983): "Path-Independent Integrals, Energy Release Rates, and General Solutions of Near-Tip Fields in Mixed-Mode Dynamic Fracture Mechanics", *Engineering Fracture Mechanics* 18-1,1-22
4. Max Mark Frocht, (1948): *Photoelasticity*, Vol.II, pp104-117, John wiley & Sons Inc.